

Self-Paced Deep Regression Forests with Consideration on Underrepresented Samples

Lili Pan, Shijie Ai, Yazhou Ren, Zenglin Xu

University of Electronic Science and Technology of China

lilipan@uestc.edu.cn, asj1995@163.com, yazhou.ren@uestc.edu.cn, zlzu@uestc.edu.cn

Abstract

Deep discriminative models (*e.g.* deep regression forests, deep Gaussian process) have been extensively studied recently to solve problems such as facial age estimation and head pose estimation. Most existing methods pursue to achieve robust and unbiased solutions through either learning more discriminative features, or weighting samples. We argue what is more desirable is to gradually learn to discriminate like our human being, and hence we resort to self-paced learning (SPL). Then, a natural question arises: *can self-paced regime guide deep discriminative models to obtain more robust and less unbiased solutions?* To this end, this paper proposes a new deep discriminative model – self-paced deep regression forests considering sample uncertainty (SPUDRFs). It builds up a new self-paced learning paradigm: easy and underrepresented samples first. This paradigm could be extended to combine with a variety of deep discriminative models. Extensive experiments on two computer vision tasks, *i.e.*, facial age estimation and head pose estimation, demonstrate the efficacy of SPUDRFs, where state-of-the-art performances are achieved.

Keywords: deep regression forests, self-paced learning, predictive uncertainty, entropy.

1. Introduction

Deep discriminative models (*e.g.* deep regression forests and deep Gaussian process) have recently been applied to many computer vision problems with remarkable success. They compute the input to output mapping for regression or classification by virtue of deep neural networks [1, 2, 3, 4]. For example, in facial age estimation, the mapping from facial features to age are computed, such that given a new face image, its corresponding age can be predicted [1, 2, 3]. In general, deep discriminative models probably achieve better performance when large amounts of effective training data are available (less noisy and imbalanced). However, such ideal data is very difficult to collect, especially when large amounts of labels are required.

Computer vision literatures are filled with scenarios in which we are required to learn a deep discriminative model, which is not only robust to confusing and

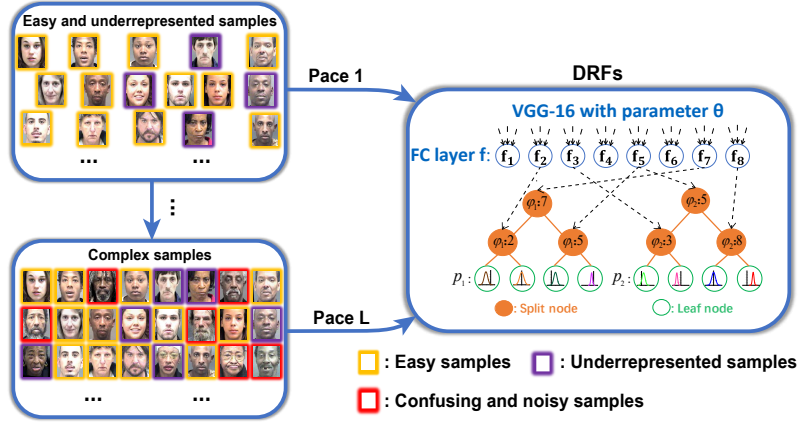


Figure 1: The illustration of SPUDRFs. It shows a new self-paced learning paradigm: easy and underrepresented samples first. This builds on the intuition that human learns what is uncertain for us again and again to gain better perception.

noisy samples, but also can conquer imbalanced training data problem [5, 6, 7]. One common approach to achieve this goal is to learn robust and discriminative vision features through rather deep neural networks, and fed these features into a *cost-sensitive* discriminative function, often with regularization [8, 9, 10, 5, 11]. The other typical approach reweights training samples according to their cost values or gradient directions (*i.e.* meta learning [12, 13, 14]). These strategies are unlike our human beings, we actually learn things gradually – start with easy concepts and build up to complex ones, and can exclude extremely hard ones. More importantly, we have a sense of *uncertainty* for some samples (*e.g.* seldom seen) and progressively improve our capability to recognize them. Thus, the main challenge towards realistic discrimination lies in mimic how the human discrimination system might work.

This line of thinking makes us resort to self-paced learning – a gradual learning regime inspired by the learning manner of humans (from easy to complex). In fact, there are rare studies on the problem of self-paced deep discriminative models. Then, a natural question arises: *can the self-paced regime guide deep discriminative models to obtain more robust and unbiased solutions?*

Motivated by this, we propose a new self-paced learning paradigm for deep discriminative models, which considers both easiness and uncertainty of samples, rendering more robust and unbiased solutions. Specifically, we focus on deep regression forests (DRFs), a typical discriminative method, and propose self-paced deep regression forests considering sample uncertainty (SPUDRFs). First, by virtue of SPL, our model distinguishes the confusing and noisy samples from regular ones, and emphasizes more on “good” samples to obtain more robust solutions. Second, our method explores to train underrepresented samples first to alleviate the biased solution problem in DRFs, which is caused by

the imbalanced training data. This builds on the intuition that humans learn what is uncertain for us again and again to gain better perception. Third, we ultimately build up a new self-paced learning paradigm for DRFs: easy and underrepresented samples first, as shown in Fig. 1, which could be extended to a variety of deep discrimination models.

For verification, we apply the SPUDRFs framework on two computer vision problems: (1) facial age estimation, and (2) head pose estimation. Extensive experimental results demonstrate the efficacy of our proposed new self-paced paradigm for deep discriminative models. Moreover, on both aforementioned problems, SPUDRFs almost achieve the state-of-the-art performance.

2. Related Work

This section reviews the deep discriminative methods for facial age estimation and head pose estimation, and SPL methods.

Facial Age Estimation. Deep discriminative model based facial age estimation, for example [10, 3, 8, 15, 16], employ DNNs to model the age mapping precisely. Ordinal-based approaches [10, 3] resort to a set of sequential binary queries – each query refers to a comparison with a predefined age, to exploit the inter-relationship (ordinal information) among age labels. Furthermore, improved deep label distribution learning (DLDL-v2) [8] explores the underlying age distribution patterns to effectively accommodate age ambiguity. Besides, deep regression forests (DRFs) [15] connect random forests to deep neural networks and achieve promising results. BridgeNet [16] uses local regressors to partition the data space and gating networks to provide continuity-aware weights. The final age estimation result is the mixture of the weighted regression results. Overall, these deep discriminative model based approaches have enhanced age estimation performance largely; however, they plausibly ignore one problem: the interference arising from confusing and noisy samples – facial images with PIE (*i.e.* pose, illumination and expression) variation, occlusion, misalignment and so forth.

Head Pose Estimation. In the field of head pose estimation, Riegler [17] utilized convolutional neural networks (CNN) for head pose estimation, which can better learn the patch features of facial images and achieve higher estimation performance. In [4], Huang *et al.* adopted multi-layer perceptron (MLP) networks for head pose estimation and proposed multi-modal deep regression networks for further performance improvement. In [18], Wang *et al.* proposed a deep coarse-to-fine network for head pose estimation. In [7], Ruiz *et al.* used a large synthetically expanded head pose dataset to train a rather deep multi-loss convolutional neural network (CNN) for head pose estimation and gained satisfied accuracy. Despite seeing much success, these methods seldom consider the imbalance training data, especially when coupled with the robustness problem.

Self-Paced Learning. The SPL is a gradual learning paradigm, which builds on the intuition that, rather than considering all training samples simultaneously, the algorithm should be presented with the training data from easy to difficult, which facilitates learning [19, 20]. Variants of SPL methods have been

proposed recently with varying degrees of success. For example, in [21], Zhao *et al.* generalized the conventional binary (hard) weighting scheme for SPL to a more effective real valued (soft) weighting manner. In [22], Ma *et al.* proposed self-paced co-training which applies self-paced learning to multi-view or multi-modality problems. In [23], Ren *et al.* introduced capped-norm into the objective of SPL, so as to further exclude the interference of noisy examples. In fact, the majority of these mentioned works can be cast as the combination of SPL and shallow classification models, where SVM and logistic regressors are usually involved. In computer vision, due to the remarkable ability of deep neural networks, some authors have realized SPL may guide deep discriminative models to achieve more robust solutions recently. In [24], Li *et al.* seek to improve CNNs with self-paced learning (SPL) for enhancing the learning robustness of CNNs. However, [24] omits one important problem in the discriminative model: the imbalance training data. In contrast to SPCNN, our SPUDRFs has three advantages: (i) it emphasizes early learning from the uncertain samples, and hence tends to achieve more unbiased solutions; (ii) it suits to more general and complex discriminative problems, especially deep regression; (iii) it creatively explore how self-paced learning integrates with deep discriminative models with a probabilistic interpretation.

Our work is inspired by the existing work [25, 26] in SPL that takes the class balance into consideration. Jiang *et al.* [26] encouraged class diversity of samples in the early stage of self-paced training. Yang *et al.* [25] defined a metric, named complexity of image category, to measure sample number and recognition difficult jointly, and adopted this measure for training sample selection in SPL. The aforementioned two methods, however, are only suited to the classification problems. In this paper, we will go further along this direction and extend to more general deep discriminative problems, particularly regression.

3. Preliminaries

In this section, we review the basic concepts of deep regression forests (DRFs) [15].

Deep Regression Tree. DRFs usually comprise a number of deep regression trees. A deep regression tree, given input-output pairs $\{\mathbf{x}_i, y_i\}_{i=1}^N$, where $\mathbf{x}_i \in \mathbb{R}^{D_x}$ and $y_i \in \mathbb{R}$, model the mapping from input to output through DNNs coupled with a regression tree, where a regression tree \mathcal{T} consists of split (or decision) nodes \mathcal{N} and leaf (or prediction) nodes \mathcal{L} [15] (see Fig. 1). More specifically, each split node $n \in \mathcal{N}$ possesses a split to determine whether a sample \mathbf{x}_i goes to the left or right subtree; each leaf node $\ell \in \mathcal{L}$ corresponds to a Gaussian distribution $p_\ell(y_i)$ with mean μ_ℓ and variance σ_ℓ^2 – parameters of output distribution defined for each tree \mathcal{T} .

Split Node. Split node has a split function, $s_n(\mathbf{x}_i; \Theta) : \mathbf{x}_i \rightarrow [0, 1]$, which is parameterized by Θ – the parameters of DNNs. Conventionally, the split function is formulated as $s_n(\mathbf{x}_i; \Theta) = \sigma(\mathbf{f}_{\varphi(n)}(\mathbf{x}_i; \Theta))$, where $\sigma(\cdot)$ is the sigmoid function, $\varphi(\cdot)$ is an index function to specify the $\varphi(n)$ -th element of $\mathbf{f}(\mathbf{x}_i; \Theta)$ in correspondence with a split node n , and $\mathbf{f}(\mathbf{x}_i; \Theta)$ denotes, given an input \mathbf{x}_i ,

the learned deep features through DNNs. An example to illustrate the sketch chart of the DRFs is shown in Fig. 1, where φ_1 and φ_2 are two index functions for the two trees. Finally, the probability of the sample \mathbf{x}_i falling into the leaf node ℓ is given by:

$$\omega_\ell(\mathbf{x}_i|\Theta) = \prod_{n \in \mathcal{N}} s_n(\mathbf{x}_i; \Theta)^{[\ell \in \mathcal{L}_{n_l}]} (1 - s_n(\mathbf{x}_i; \Theta))^{[\ell \in \mathcal{L}_{n_r}]}, \quad (1)$$

where $[\mathcal{H}]$ denotes an indicator function conditioned on the argument \mathcal{H} . In addition, \mathcal{L}_{n_l} and \mathcal{L}_{n_r} correspond to the sets of leaf nodes owned by the subtrees \mathcal{T}_{n_l} and \mathcal{T}_{n_r} rooted at the left and right children n_l and n_r of node n , respectively. **Leaf Node.** For tree \mathcal{T} , given \mathbf{x}_i , each leaf node $\ell \in \mathcal{L}$ defines a predictive distribution over age y_i , denoted by $p_\ell(y_i)$. To be specific, $p_\ell(y_i)$ is assumed to be a Gaussian distribution: $\mathcal{N}(y_i|\mu_\ell, \sigma_\ell^2)$. Thus, considering all leaf nodes, the final distribution of y_i conditioned on \mathbf{x}_i is averaged by the probability of reaching each leaf:

$$p_{\mathcal{T}}(y_i|\mathbf{x}_i; \Theta, \pi) = \sum_{\ell \in \mathcal{L}} \omega_\ell(\mathbf{x}_i|\Theta) p_\ell(y_i), \quad (2)$$

where Θ and π represent the parameters of DNNs and the distribution parameters $\{\mu_\ell, \sigma_\ell^2\}$, respectively. It can be viewed as a mixture distribution, where $\omega_\ell(\mathbf{x}_i|\Theta)$ denotes mixing coefficients and $p_\ell(y_i)$ denotes sub-modal distributions. One note that the distribution parameters vary along with tree \mathcal{T}_k , and thus we rewrite them in terms of π_k .

Forests of Regression Trees. Since a forest comprises a set of deep regression trees $\mathcal{F} = \{\mathcal{T}_1, \dots, \mathcal{T}_K\}$, the predictive output distribution, given \mathbf{x}_i , is obtained by averaging over all trees:

$$p_{\mathcal{F}}(y_i|\mathbf{x}_i, \Theta, \Pi) = \frac{1}{K} \sum_{k=1}^K p_{\mathcal{T}_k}(y_i|\mathbf{x}_i; \Theta, \pi_k), \quad (3)$$

where K is the number of trees and $\Pi = \{\pi_1, \dots, \pi_K\}$. $p_{\mathcal{F}}(y_i|\mathbf{x}_i, \Theta, \Pi)$ can be viewed as the likelihood that the i^{th} sample has output y_i .

4. Self-Paced DRFs with Consideration on Underrepresented Samples

The obviously observed problems in training deep discriminative model in computer vision tasks lie in: (1) the noisy and confusing samples, and (2) the imbalanced training data (see Fig. 2). This first problem is due to the lighting condition changes, image noise, pose, occlusion, and so forth in visual data capturing. For example, in facial age estimation, there exist facial images with PIE (*i.e.* pose, illumination and expression) variation, occlusion, and misalignment. The latter problem is mainly caused by the natural distribution of visual data. For example, in age data, the persons with especially old ages tend to be scarce. The mentioned problems have been studied in vast recent works [27, 28] as how

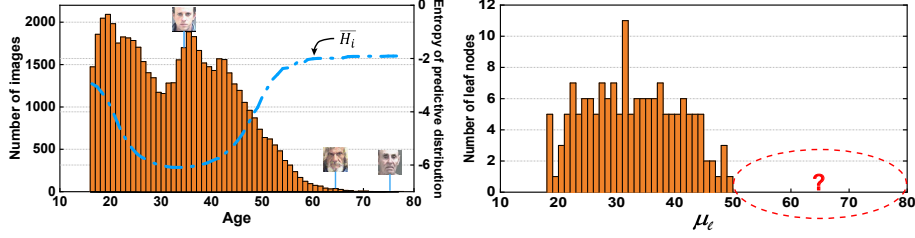


Figure 2: The Motivation of considering underrepresented samples in DRFs. **Left:** The histogram shows the number of face images at different ages, and the average entropy curve represents the predictive uncertainty. We observe the high entropy values correspond to *underrepresented samples*. **Right:** The distribution of the means of all leaf nodes reveals the underrepresented samples (probably with high predictive uncertainty) are usually ignored at the very start, incurring the final biased results.

to learn more discriminative features or how to reweight samples. However, we argue what is more desirable is to discriminate like our human beings.

Intuitively inspired by the gradual learning process of humans, which can conquer the above two problems to some extent. We resort to self-paced learning, which builds on the intuition that, rather than considering all training samples simultaneously, the model should be trained with the training data from easy to difficult. By virtue of this strategy, the deep discriminative models tend to obtain more robust solutions, as such a strategy emphasizes more on “good” samples. However, in the self-paced process, one potential problem we observe is that the underrepresented samples (with high predictive uncertainty) are usually ignored at the very start, incurring the final biased results (see Fig. 2).

To solve this problem, we propose a new self-paced deep discriminative model considering sample uncertainty meanwhile. The model, named SPU-DRFs, starts learning with the easy yet underrepresented samples, and build up to complex ones, as illustrated in Fig. 1. The easy and underrepresented samples are chosen for training in our DRFs at a very early start. This leads to solutions which are less biased, which will be seen in our experiment part (see Sec. 4.3).

4.1. Sample Uncertainty

Given the sample \mathbf{x}_i , the uncertainty for this sample can be measured by the entropy of its predictive output distribution $p_{\mathcal{F}}(y_i|\mathbf{x}_i, \Theta, \Pi)$:

$$H[p_{\mathcal{F}}(y_i|\mathbf{x}_i, \Theta, \Pi)] = \frac{1}{K} \sum_{k=1}^K H[p_{\mathcal{T}_k}(y_i|\mathbf{x}_i, \Theta, \pi_k)], \quad (4)$$

where

$$H[p_{\mathcal{T}_k}(y_i|\mathbf{x}_i, \Theta, \pi_k)] = - \int p_{\mathcal{T}_k}(y_i|\mathbf{x}_i, \Theta, \pi_k) \ln p_{\mathcal{T}_k}(y_i|\mathbf{x}_i, \Theta, \pi_k) dy_i, \quad (5)$$

which corresponds to the k^{th} tree. The larger the entropy is, the more uncertain the prediction should be. As previously discussed, $p_{\mathcal{T}_k}(y_i|\mathbf{x}_i; \Theta, \pi_k)$ can be treated as a mixture distribution $\frac{1}{K} \sum_{k=1}^K p_{\mathcal{T}_k}(y_i|\mathbf{x}_i; \Theta, \pi_k)$, where $\omega_\ell(\mathbf{x}_i|\Theta)$ denotes mixing coefficients and $p_\ell(y_i)$ denotes sub-modal distributions. Thus, substituting the mixture distribution back into the entropy calculation will result in the following equation:

$$H[p_{\mathcal{T}_k}(y_i|\mathbf{x}_i, \Theta, \pi_k)] = \sum_{\ell \in \mathcal{L}} \left\{ \ln \omega_\ell(\mathbf{x}_i|\Theta) + \frac{1}{2} \ln(2\pi\sigma_\ell^2) + \frac{1}{2} \right\}. \quad (6)$$

The underrepresented samples are often scarce, and have not been treated fairly, resulting in large prediction uncertainty (*i.e.* entropy).

4.2. Objective Functions

Rather than considering all the samples simultaneously in existing deep discriminative models, our proposed SPUDRFs presented with the training data in a meaningful order, that is, easy and uncertain samples first. For this purpose, we shall define a latent variable v_i that indicates whether the i^{th} sample is selected ($v_i = 1$) or not ($v_i = 0$) depending on how easy and uncertain it is for training. Our objective is to jointly maximize the log likelihood function with respect to DRFs parameters Θ and Π , and learn the latent selecting variables $\mathbf{v} = (v_1, \dots, v_N)^T$. On the other hand, we prefer to select the underrepresented samples, which probably have higher predictive uncertainty (*i.e.* entropy), particularly in the early pace. It builds on the intuition that humans learn what is uncertain for us again and again so as to gain better perception. Therefore, we maximize a self-paced term regularized likelihood function, meanwhile considering more on underrepresented samples,

$$\max_{\Theta, \Pi, \mathbf{v}} \sum_{i=1}^N v_i \{ \log p_{\mathcal{F}}(y_i|\mathbf{x}_i, \Theta, \Pi) + \gamma H_i \} + \lambda \sum_{i=1}^N v_i, \quad (7)$$

where λ is a parameter controlling the learning pace, γ is the parameters imposing on uncertainty, and H_i denotes the predictive uncertainty of the i^{th} sample, as previously discussed in Sec. 4.1. When γ decays to 0, the objective function is equivalent to the log likelihood function with respect to DRFs parameters Θ and Π . Eq. (7) indicates each sample is weighted by v_i , and whether $\log p_{\mathcal{F}}(y_i|\mathbf{x}_i, \Theta, \Pi) + \gamma H_i > -\lambda$ determines the i^{th} sample is selected or not. That is, the sample with high likelihood value or high predictive uncertainty may be selected. The optimal v_i^* is:

$$v_i^* = \begin{cases} 1 & \text{if } \log p_{\mathcal{F}} + \gamma H_i > -\lambda \\ 0 & \text{otherwise} \end{cases}, \quad (8)$$

where $p_{\mathcal{F}}(y_i|\mathbf{x}_i, \Theta, \Pi)$ is denoted by $p_{\mathcal{F}_i}$ for simplicity.

Iteratively increasing λ and decreasing γ , samples are dynamically involved in the training of DRFs, starting with easy and underrepresented samples and

ending up with all samples. Note every time we retrain DRFs, that is, maximizing Eq. (7), our model is initialized to the results of the last iteration. As such, our model is initialized progressively by the result of the previous pace – adaptively calibrated by “good” samples. This also means we place more emphasis on easy and underrepresented samples rather than confusing and noisy ones. Thus, SPUDRFs are prone to have more robust and less biased solutions since we adequately consider the underrepresented samples.

4.2.1. Mixture Weighting.

As mentioned previously, the above approach performs a hard assignment of data points to paces, in which a sample is either selected ($v_i = 1$) or not ($v_i = 0$). Such a weighting scheme appears to be less appropriate as it omits the importance of samples. To alleviate this problem, we adopt a mixture weighting scheme, which is a hybrid of hard and soft weighting. As we know, soft weighting assigns real-valued weights (which reflect importance) to each sample. The objective function with the mixture weighting scheme is defined as:

$$\max_{\Theta, \Pi, \mathbf{v}} \sum_{i=1}^N v_i \{ \log p_{\mathcal{F}}(y_i | \mathbf{x}_i, \Theta, \Pi) + \gamma H_i \} + \zeta \sum_{i=1}^N \log(v_i + \zeta/\lambda), \quad (9)$$

where $\zeta = (\frac{1}{\lambda'} - \frac{1}{\lambda})^{-1}$ and $\lambda > \lambda' > 0$. The self-paced regularizer in Eq. (9) is convex with respect to $v \in [0, 1]$. Then, setting the partial gradient of Eq. (9) with respect to v_i as zero will lead to the following:

$$\log p_{\mathcal{F}}(y_i | \mathbf{x}_i, \Theta, \Pi) + \gamma H_i + \frac{\zeta}{v_i + \zeta/\lambda} = 0. \quad (10)$$

The optimal solution of v_i is given by:

$$v_i^* = \begin{cases} 1 & \text{if } \log p_{\mathcal{F}} + \gamma H_i \geq -\lambda' \\ 0 & \text{if } \log p_{\mathcal{F}} + \gamma H_i \leq -\lambda \\ \frac{-\zeta}{\log p_{\mathcal{F}} + \gamma H_i} - \zeta/\lambda & \text{otherwise} \end{cases} \quad (11)$$

If either the likelihood or the predictive uncertainty (defined for distinguishing underrepresented samples) is too large, v_i^* equals to 1. In addition, if the likelihood and the predictive uncertainty are both too small, v_i^* equals to 0. Except the above two situations, the soft weighting calculation (i.e., the last line of Eq. (11)) is adopted.

4.2.2. Curriculum Reconstruction.

The underrepresented samples play an important role in our SPUDRFs algorithm. As previously mentioned, the proposed new self-paced regime coupled with a mixture weighting scheme emphasizes more on underrepresented samples, rendering better solutions. However, the intrinsic reason that causes predictive uncertainty plausibly is the imbalanced training data. Towards this line of thinking, we re-balance data distribution via a curriculum reconstruction strategy. More specifically, we distinguish the underrepresented samples (whose H_i is larger than β) from regular ones at each pace, and augment them into the training data.

4.3. Optimization

We propose a two-step alternative search strategy (ASS) algorithm to solve the optimization problem of SPUDRFs: (i) update \mathbf{v} for sample selection with fixed Θ and Π , and (ii) update Θ and Π with current fixed sample weights \mathbf{v} . **Optimizing Θ and Π .** The parameters $\{\Theta, \Pi\}$ and weights \mathbf{v} are optimized alternatively. With fixed \mathbf{v} , our DRFs is learned by alternatively updating Θ and Π . In [15], the parameters Θ for split nodes (*i.e.* parameters for VGG) is updated through gradient descent since the loss is differentiable with respect to Θ . While the parameters Π for leaf nodes are updated by virtue of variational bounding [15] when fixing Θ .

Optimizing \mathbf{v} . As previously mentioned, v_i is a binary variable or real variable ranged in $[0, 1]$. It indicates how to weight the i^{th} sample during training. The parameter λ could be initialized to obtain 50% samples to train the model, and is then progressively increased to involve 10% more data in each pace. The parameter γ could be initialized empirically and is progressively decayed to zero. The training stops when all the samples are selected, at $\gamma = 0$. Along with increasing λ and decreasing γ , DRFs are trained to be more “mature”. This learning process is like how our human beings learn one thing from easy and uncertain to complex.

5. Experimental Results

5.1. Tasks and Benchmark Datasets

Age Estimation. The Morph II [29] dataset contains 55,134 unique face images of 13618 individuals with unbalanced gender and ethnicity distributions, is a large and the most popular publicly available real age dataset. The FG-NET [30] dataset includes 1,002 color and grey images of 82 people with each subject almost accompanied by more than 10 photos at different ages. Since all images were taken in a totally uncontrolled environment, there exists a large deviation on lighting, pose and expressions of the images inside the dataset.

Head Pose Estimation. The BIWI dataset [31] contains 20 subjects which 10 are male and 6 are female, furthermore, 4 males have been chosen twice with wearing glasses or not. It includes 15678 images collected by a Kinect sensor device for different persons and head poses with pitch, yaw and roll angles mainly ranging within $\pm 60^\circ$, $\pm 75^\circ$ and $\pm 50^\circ$.

5.2. Experimental Setup

5.2.1. Dataset Setting

The settings of different datasets are given below.

- **Morph II.** Following the recent relevant work [15], the images in Morph II were divided into two sets: 80% for training and the rest 20% for testing. The random division was repeated 5 times and the reported performance was averaged over these 5 times. The VGG-Face [9] networks were chosen as the pre-trained model.

- **FGNET.** The leave-one-person-out scheme [15] was adopted, where the images of one person were selected for testing and the remains for training. The VGG-16 networks were pre-trained on the IMDB-WIKI [5] dataset.
- **BIWI.** Similarly, 80% of the whole data was randomly chosen for training and the rest 20% for testing, and this operation was repeated 5 times. Moreover, the VGG-FACE networks were the pre-trained model.

5.2.2. Evaluation Metrics.

The mean absolute error (MAE) is the average absolute error between the ground truth and the predicted output: $\sum_{i=1}^N |\hat{y}_i - y_i| / N$, \hat{y}_i represents the estimated output of the i^{th} sample, and N is the total number of testing images. The cumulative score (CS) denotes the percentage of images sorted in the range of $[y_i - L, y_i + L]$: $CS(L) = \sum_{i=1}^N [\hat{y}_i - y_i \leq L] \cdot 100\% / N$, where $[\cdot]$ denotes an indicator function and L is the error range.

5.2.3. Preprocessing and Data Augmentation.

On the Morph II and FG-NET datasets, MTCNN [32] was used for joint face detection and alignment. Furthermore, following [15], we augmented training images in three ways: 1) random cropping; 2) adding Gaussian noise; 3) a random horizontal flipping. On the BIWI dataset, we utilized the depth images for training.

5.2.4. Parameters Setting.

The VGG-16 [33] was employed as the fundamental backbone networks of SPUDRFs. The hyper-parameters of VGG-16 were: training batch size (32 on Morph II and BIWI, 8 for FG-NET), drop out ratio (0.5), max iterations of each pace (80k on Morph II, 20k on FG-NET, and 40k on BIWI), stochastic gradient descent (SGD), initial learning rate (0.2 on Morph II, 0.1 on BIWI, 0.02 on FG-NET) by reducing the learning rate ($\times 0.5$) per 10k iterations. The hyper-parameters of SPUDRFs were: tree number (5), tree depth (6), output unit number of feature learning (128).

5.3. Validity of Our Proposed Method

5.3.1. Self-paced Learning Strategy.

The validity of self-paced strategy for learning deep discriminative models is mainly demonstrated by the following DRFs experiments on the MorphII dataset. We first used all training images in the Morph II datasets to train DRFs for ranking samples at the beginning pace. In the first pace, 50% easy and uncertain samples were selected for training. Here, $\gamma = 15$, and λ was set to guarantee the first 50% samples with large $\log p_{\mathcal{F}_i} + \gamma H_i$ values were involved. Retraining proceeded with progressively increasing λ such that every 1/9 of the rest data was gradually involved at each pace, where γ was decreased by 10%. In the last pace, the value γ was constrainedly set to be 0. The visualization of this process can be found in Fig. 3.

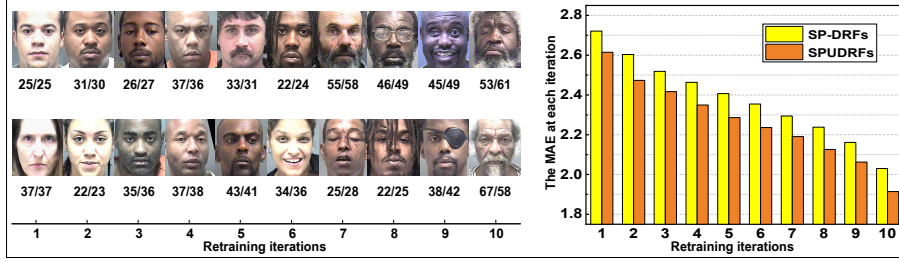


Figure 3: The gradual learning process of SP-DRFs and SPUDRFs. **Left:** The typical worst cases at each iteration become more confusing and noisy along with iteratively increase λ and decreasing γ . The two numbers below each image are the real age (left) and predicted age (right). **Right:** The MAEs of SP-DRFs and SPUDRFs at each pace descends gradually. The SPUDRFs show its superiority of taking predictive uncertainty into consideration, when compared with SP-DRFs.

Fig. 3 illustrates the representative face images at each learning pace of SPUDRFs, along with increasing λ and decreasing γ . The two numbers below each image are the real age (left) and predicted age (right). We observe that the training images in the later paces are obviously more confusing and noisy than the ones in the early paces. Since our model is initialized by the results of the last retraining pace, meaning adaptively calibrated by “good” samples rather than confusing and noisy ones. As a result, it has improved performance than DRFs, where the MAE is promoted from 2.17 to 1.91, and the CS is improved from 92.79% to 91.31% (see Fig. 5(a)).

Fig. 3 also shows the comparison between SP-DRFs and SPUDRFs on the Morph II datasets. The yellow bar denotes the MAEs of SP-DRFs, while the orange bar denotes for SPUDRFs. We find the MAEs of SPUDRFs are lower than SP-DRFs at each pace, particularly the last pace (1.91 against 2.02). As we discussed previously in Fig. 2, SPUDRFs are prone to reach more unbiased solutions due to the wider covering range of leaf nodes, owing to considering sample uncertainty.

5.3.2. Considering Underrepresented Samples.

The effect of considering Underrepresented samples in self-paced deep discriminative model – DRFs is further demonstrated on the BIWI dataset. In DRFs, we similarly utilized all the training data to learn DRFs and rank the samples according to this result for the first pace. In the first pace, the top 50% “good” images, with high $\log p_{\mathcal{F}_i} + \gamma H_i$ values are selected for retraining. The value of γ was initialized as 15. Subsequently, every 10% of the rest data was progressively involved for retraining at each pace by virtue of changing λ . γ was progressively decreased until zero. In DRFs, we adopted the same self-paced strategy as in SPUDRFs, but without considering the underrepresented sample.

Fig. 4 visualizes the leaf node distributions of SP-DRFs and SPUDRFs in the progressive learning. The Gaussian means μ_l associated with the 160 leaf nodes,

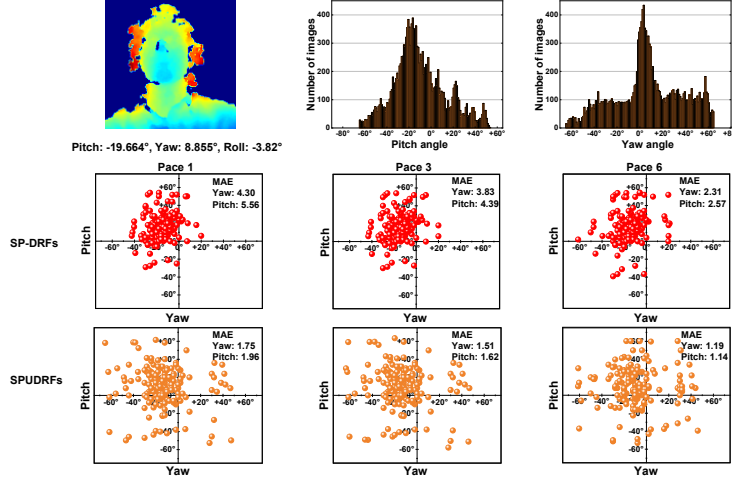


Figure 4: The leaf node distribution of SP-DRFs and SPUDRFs in gradual learning process. Three paces, *i.e.* pace 1, 3, and 6, are randomly chosen for visualization. For SP-DRFs, the Gaussian means of leaf nodes (the red points in the second row) are concentrated in a small range, incurring seriously biased solutions. For SPUDRFs, the Gaussian means of leaf nodes (the orange points in the third row) distribute widely, leading to much better MAE performance.

where each 32 leaf nodes are defined for 5 trees, are plotted in each sub-figures. Three paces, *i.e.* pace 1, 3, and 6, are randomly chosen for visualization. Only pitch and yaw angles are shown for clarity. Besides, the original distribution of pitch and yaw angles associated with all images in BIWI are also shown.

In Fig. 4, the comparison results between SP-DRFs and SPUDRFs demonstrate the efficacy of considering underrepresented samples in self-paced learning framework. For SP-DRFs, where no predictive uncertainty has been considered, the Gaussian means of leaf nodes (red points in the second row) are concentrated in a small range, incurring seriously biased solutions. That means the scarce samples have not been treated fairly. The poor MAEs are the evidence for this, which are even inferior to DRFs (see Fig. 7(a)). As our SPUDRFs model chooses the uncertain samples (*i.e.* usually scarce) for training at a very early pace, it prone to achieve less unbiased solutions. This can be demonstrated by the relatively wider distribution of leaf nodes, and also the much lower MAEs, as shown in the third row of Fig. 4.

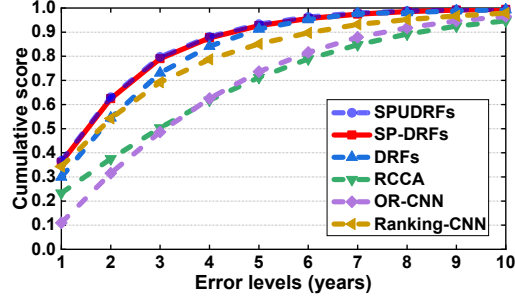
5.4. Comparison with State-of-the-art Methods

We compared our SPUDRFs with other state-of-the-art methods on Morph II dataset, FG-NET dataset and BIWI dataset.

Results on Morph II. Fig. 5(a) compares the performance of SPUDRFs with other baseline methods: LSVR [34], RCCA [35], OHRank [36], OR-CNN [10], Ranking-CNN [3], DRFs [15], and DLDL-v2 [8]. Firstly, owing to the significant

Method	MAE↓	CS↑
LSVR [34]	4.31	66.2%
RCCA [35]	4.25	71.2%
OHRank [36]	3.82	N/A
OR-CNN [10]	3.27	73.0%
Ranking-CNN [3]	2.96	85.0%
DRFs [15]	2.17	91.3%
DLDL-v2 [8]	1.97	N/A
SP-DRFs	2.02	92.79%
SPUDRFs	1.91	93.31%

(a)

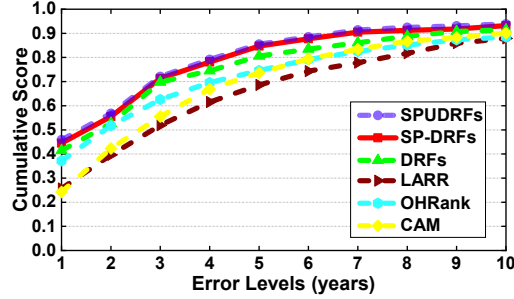


(b)

Figure 5: The comparison results on the Morph II dataset: (a) The MAE comparison with the state-of-the-art methods, (b) the CS curves of the comparison methods.

Method	MAE↓	CS↑
IIS-LDL [37]	5.77	N/A
LARR [38]	5.07	68.9%
MTWGP [39]	4.83	72.3%
DIF [40]	4.80	74.3%
OHRank [36]	4.48	74.4%
CAM [41]	4.12	73.5%
DRFs [15]	3.06	83.33%
SP-DRFs	2.84	84.73%
SPUDRFs	2.77	85.53%

(a)



(b)

Figure 6: The comparison results on the FGNET II dataset: (a) The MAE comparison with the state-of-the-art methods, (b) the CS curves of the comparison methods.

feature extraction ability of DNNs, the SPUDRFs method is much superior to the shallow model based approaches, such as LSVR [34] and OHRank [36]. Secondly, our SPUDRFs outperform other deep discriminative methods, which is due to its valid self-paced regime, thereby leading to more robust and less unbiased solutions. Thirdly, SPUDRFs outperform SP-DRFs on both MAE and CS, and achieve state-of-the-art performance. Fig. 5(b) shows the CS comparison on this dataset. We observe that the CS of SPUDRFs reached 93.31% at error level $L = 5$, which was significantly better than DRFs and obtained 2.01% increment.

Results on FG-NET. Fig. 6(a) shows comparison results of SPUDRFs with the state-of-the-art approaches on FGNET dataset. As can be seen, SPUDRFs reaches an MAE of 2.77 years, which reduces the performance of DRFs by 0.29 years. Besides, the CS comparisons are shown in Fig. 6(b), SPUDRFs consistently outperform other recent proposed methods at different error levels, proving that our method is effective in enhancing the robustness of facial age estimation.

Results on BIWI. Fig. 7(a) shows the comparison results of our methods

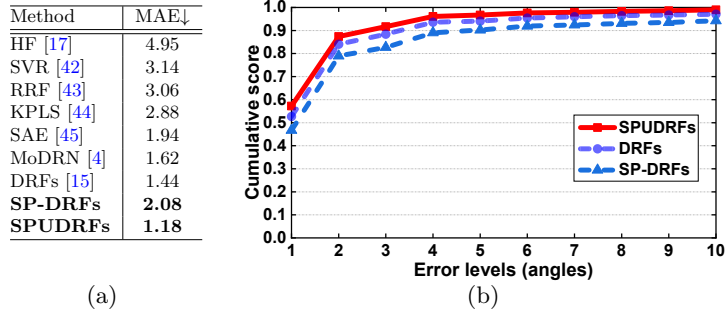


Figure 7: The comparison results on the BIWI dataset: (a) The MAE comparison with the state-of-the-art methods, (b) the CS curves the comparison methods.

with several state-of-the-art approaches. The experimental results reveal the proposed SPUDRFs method achieves the best performance with an MAE of 1.18, which is state-of-the-art. *Besides, we observe one important phenomenon: the MAE of SP-DRFs is even much worse than DRFs. This further demonstrates the obvious drawback of the selection scheme in original SPL – incurring seriously biased solutions.* As we illustrated in Fig. 4, in the first pace of SPL, the Gaussian means of leaf nodes are concentrated in a small range, leading a biased result. By virtue of incorporating uncertain samples in the early pace, SPUDRFs are prone to alleviate the above problems, with a more rational distribution of the leaf nodes. Fig. 7(b) plots only three CS curves for brevity, *i.e.*, DRFs, SP-DRFs and SPUDRFs, which is the average of the three angles. Our SPUDRFs also outperform DRFs and SP-DRFs at different error levels.

6. Conclusion and Future Work

This paper explored how self-paced regime guided deep discriminative models to obtain more robust and less unbiased solutions on different computer vision tasks (*e.g.* facial age estimation and head pose estimation). Specifically, a novel self-paced paradigm, which starts with easy and underrepresented samples and build up to complex ones, was proposed. Such a paradigm was applied to a typical deep regression model – deep regression forests (DRFs), and lead to a new model, namely deep regression forests with consideration on underrepresented samples (SPUDRFs). Moreover, a new mixture weighting scheme in self-paced learning which jointly considers sample loss and predictive uncertainty was proposed. Extensive experiments on two well-known computer vision tasks demonstrated the efficacy of the proposed new self-paced paradigm. The future work will include exploring how to combine the new paradigm with other deep discriminative models.

References

- [1] S. Chen, C. Zhang, M. Dong, Deep age estimation: From classification to ranking, *IEEE Transactions on Multimedia* 20 (8) (2018) 2209–2222.
- [2] C. Yan, C. Lang, W. Tao, X. Du, Z. Chen, Age estimation based on convolutional neural network, in: *Pacific Rim Conference on Multimedia*, 2014, pp. 211–220.
- [3] S. Chen, C. Zhang, M. Dong, J. Le, M. Rao, Using Ranking-CNN for age estimation, in: *IEEE Conference on Computer Vision and Pattern Recognition*, 2017, pp. 742–751.
- [4] Y. Huang, L. Pan, Y. Zheng, M. Xie, Mixture of deep regression networks for head pose estimation, in: *IEEE International Conference on Image Processing*, IEEE, 2018, pp. 4093–4097.
- [5] R. Rothe, R. Timofte, L. Van Gool, Deep expectation of real and apparent age from a single image without facial landmarks, *International Journal of Computer Vision* 126 (2-4) (2018) 144–157.
- [6] D. Huang, L. Han, F. De la Torre, Soft-margin mixture of regressions, in: *IEEE Conference on Computer Vision and Pattern Recognition*, 2017, pp. 4058–4066.
- [7] N. Ruiz, E. Chong, J. M. Rehg, Fine-grained head pose estimation without keypoints, in: *Proceedings of the IEEE conference on computer vision and pattern recognition workshops*, 2018, pp. 2074–2083.
- [8] B.-B. Gao, H.-Y. Zhou, J. Wu, X. Geng, Age estimation using expectation of label distribution learning, in: *International Joint Conference on Artificial Intelligence*, 2018, pp. 712–718.
- [9] O. M. Parkhi, A. Vedaldi, A. Zisserman, Deep face recognition.
- [10] Z. Niu, M. Zhou, L. Wang, X. Gao, G. Hua, Ordinal regression with multiple output CNN for age estimation, in: *IEEE Conference on Computer Vision and Pattern Recognition*, 2016, pp. 4920–4928.
- [11] E. Agustsson, R. Timofte, L. Van Gool, Anchored regression networks applied to age estimation and super resolution, in: *Proceedings of the IEEE International Conference on Computer Vision*, 2017, pp. 1643–1652.
- [12] M. Ren, W. Zeng, B. Yang, R. Urtasun, Learning to reweight examples for robust deep learning, *arXiv preprint arXiv:1803.09050*.
- [13] Y. Cui, M. Jia, T.-Y. Lin, Y. Song, S. Belongie, Class-balanced loss based on effective number of samples, in: *Proceedings of the IEEE Conference on Computer Vision and Pattern Recognition*, 2019, pp. 9268–9277.

- [14] S. Khan, M. Hayat, S. W. Zamir, J. Shen, L. Shao, Striking the right balance with uncertainty, in: *Proceedings of the IEEE Conference on Computer Vision and Pattern Recognition*, 2019, pp. 103–112.
- [15] W. Shen, Y. Guo, Y. Wang, K. Zhao, B. Wang, A. Yuille, Deep regression forests for age estimation, in: *IEEE Conference on Computer Vision and Pattern Recognition*, 2018, pp. 2304–2313.
- [16] W. Li, J. Lu, J. Feng, C. Xu, J. Zhou, Q. Tian, Bridgenet: A continuity-aware probabilistic network for age estimation, in: *IEEE Conference on Computer Vision and Pattern Recognition*, 2019, pp. 1145–1154.
- [17] G. Riegler, D. Ferstl, M. R  ther, H. Bischof, Hough networks for head pose estimation and facial feature localization, *Journal of Computer Vision* 101 (3) (2013) 437–458.
- [18] Y. Wang, W. Liang, J. Shen, Y. Jia, L.-F. Yu, A deep coarse-to-fine network for head pose estimation from synthetic data, *Pattern Recognition* 94 (2019) 196–206.
- [19] M. P. Kumar, B. Packer, D. Koller, Self-paced learning for latent variable models, in: *International Conference on Neural Information Processing Systems*, 2010, pp. 1189–1197.
- [20] D. Meng, Q. Zhao, L. Jiang, A theoretical understanding of self-paced learning, *Information Sciences* 414 (2017) 319–328.
- [21] L. Jiang, D. Meng, Q. Zhao, S. Shan, A. G. Hauptmann, Self-paced curriculum learning, in: *AAAI Conference on Artificial Intelligence*, 2015, pp. 2694–2700.
- [22] F. Ma, D. Meng, Q. Xie, Z. Li, X. Dong, Self-paced co-training, in: *Proceedings of the 34th International Conference on Machine Learning*, 2017, pp. 2275–2284.
- [23] Y. Ren, X. Yan, Z. Hu, Z. Xu, Self-paced multi-task multi-view capped-norm clustering, in: *International Conference on Neural Information Processing*, Springer, 2018, pp. 205–217.
- [24] H. Li, M. Gong, Self-paced convolutional neural networks, in: *Proceedings of the Twenty-Sixth International Joint Conference on Artificial Intelligence*, 2017, pp. 2110–2116.
- [25] J. Yang, X. Wu, J. Liang, X. Sun, M.-M. Cheng, P. L. Rosin, L. Wang, Self-paced balance learning for clinical skin disease recognition, *IEEE transactions on neural networks and learning systems*.
- [26] L. Jiang, D. Meng, S.-I. Yu, Z. Lan, S. Shan, A. Hauptmann, Self-paced learning with diversity, in: *Advances in Neural Information Processing Systems*, 2014, pp. 2078–2086.

- [27] A. Kortylewski, B. Egger, A. Schneider, T. Gerig, A. Morel-Forster, T. Vetter, Analyzing and reducing the damage of dataset bias to face recognition with synthetic data, in: The IEEE Conference on Computer Vision and Pattern Recognition (CVPR) Workshops, 2019.
- [28] V. Muthukumar, Color-theoretic experiments to understand unequal gender classification accuracy from face images, in: The IEEE Conference on Computer Vision and Pattern Recognition (CVPR) Workshops, 2019.
- [29] K. Ricanek, T. Tesafaye, Morph: A longitudinal image database of normal adult age-progression, in: 7th International Conference on Automatic Face and Gesture Recognition (FGR06), IEEE, 2006, pp. 341–345.
- [30] G. Panis, A. Lanitis, N. Tsapatsoulis, T. F. Cootes, Overview of research on facial ageing using the fg-net ageing database, *Iet Biometrics* 5 (2) (2016) 37–46.
- [31] G. Fanelli, M. Dantone, J. Gall, A. Fossati, L. Van Gool, Random forests for real time 3d face analysis, *International journal of computer vision* 101 (3) (2013) 437–458.
- [32] K. Zhang, Z. Zhang, Z. Li, Y. Qiao, Joint face detection and alignment using multi-task cascaded convolutional networks, *IEEE Signal Processing Letters* 23 (10) (2016) 1499–1503.
- [33] K. Simonyan, A. Zisserman, Very deep convolutional networks for large-scale image recognition, *arXiv* 1409.1556.
- [34] G. Guo, G. Mu, Y. Fu, T. S. Huang, Human age estimation using bio-inspired features, in: IEEE Conference on Computer Vision and Pattern Recognition, 2009, pp. 112–119.
- [35] I. Huerta, C. Fernandez, A. Prati, Facial age estimation through the fusion of texture and local appearance descriptors, in: European Conference on Computer Vision, 2014, pp. 667–681.
- [36] K. Y. Chang, C. S. Chen, Y. P. Hung, Ordinal hyperplanes ranker with cost sensitivities for age estimation, in: IEEE Conference on Computer Vision and Pattern Recognition, 2011, pp. 585–592.
- [37] X. Geng, C. Yin, Z.-H. Zhou, Facial age estimation by learning from label distributions, *IEEE Transactions on Pattern Analysis and Machine Intelligence* 35 (10) (2013) 2401–2412.
- [38] G. Guo, Y. Fu, C. Dyer, T. Huang, Image-based human age estimation by manifold learning and locally adjusted robust regression, *IEEE Transactions on Image Processing* 17 (7) (2008) 1178–1188.
- [39] Z. Yu, D. Y. Yeung, Multi-task warped gaussian process for personalized age estimation, in: IEEE Conference on Computer Vision and Pattern Recognition, 2010, pp. 2622–2629.

- [40] H. Han, C. Otto, X. Liu, A. K. Jain, Demographic estimation from face images: Human vs. machine performance, *IEEE Transactions on Pattern Analysis and Machine Intelligence* 37 (6) (2015) 1148–1161.
- [41] K. Luu, K. Seshadri, M. Savvides, T. D. Bui, C. Y. Suen, Contourlet appearance model for facial age estimation, in: *International Joint Conference on Biometrics*, 2013, pp. 1–8.
- [42] H. Drucker, C. J. Burges, L. Kaufman, A. J. Smola, V. Vapnik, Support vector regression machines, in: *Advances in neural information processing systems*, 1997, pp. 155–161.
- [43] A. Liaw, M. Wiener, et al., Classification and regression by randomforest, *R news* 2 (3) (2002) 18–22.
- [44] M. Al Haj, J. Gonzalez, L. S. Davis, On partial least squares in head pose estimation: How to simultaneously deal with misalignment, in: *2012 IEEE Conference on Computer Vision and Pattern Recognition*, IEEE, 2012, pp. 2602–2609.
- [45] G. E. Hinton, R. R. Salakhutdinov, Reducing the dimensionality of data with neural networks, *science* 313 (5786) (2006) 504–507.